



**HAL**  
open science

## Cancer cell sonoporation at low acoustic amplitudes

Anthony Delalande, Spiros Kotopoulos, Chantal Pichon, Michiel Postema

► **To cite this version:**

Anthony Delalande, Spiros Kotopoulos, Chantal Pichon, Michiel Postema. Cancer cell sonoporation at low acoustic amplitudes. 18th International Congress on Sound and Vibration, Rio de Janeiro, Brazil, 10-14 July 2011, Jul 2011, Rio de Janeiro, Brazil. pp.1695-1702. hal-03195599

**HAL Id: hal-03195599**

**<https://hal.science/hal-03195599>**

Submitted on 11 Apr 2021

**HAL** is a multi-disciplinary open access archive for the deposit and dissemination of scientific research documents, whether they are published or not. The documents may come from teaching and research institutions in France or abroad, or from public or private research centers.

L'archive ouverte pluridisciplinaire **HAL**, est destinée au dépôt et à la diffusion de documents scientifiques de niveau recherche, publiés ou non, émanant des établissements d'enseignement et de recherche français ou étrangers, des laboratoires publics ou privés.

# CANCER CELL SONOPORATION AT LOW ACOUSTIC AMPLITUDES

Anthony Delalande

*Centre de Biophysique Moléculaire, UPR 4301 CNRS affiliated to the University of Orléans, rue Charles Sadron, 45071 Orléans Cedex 2, France*

Spiros Kotopoulos

*Department of Engineering, The University of Hull, Cottingham Road, Kingston upon Hull HU6 7RX, United Kingdom*

*email: S.Kotopoulos@2005.hull.ac.uk*

Chantal Pichon

*Centre de Biophysique Moléculaire, UPR 4301 CNRS affiliated to the University of Orléans, rue Charles Sadron, 45071 Orléans Cedex 2, France*

Michiel Postema

*Department of Physics and Technology, University of Bergen, Allégaten 55, 5007 Bergen, Norway,*

*Department of Engineering, The University of Hull, Cottingham Road, Kingston upon Hull HU6 7RX, United Kingdom, and*

*Centre de Biophysique Moléculaire, UPR 4301 CNRS affiliated to the University of Orléans, rue Charles Sadron, 45071 Orléans Cedex 2, France*

In this study we investigated the physical mechanisms of sonoporation, in order to understand and improve ultrasound-assisted drug and gene delivery. Sonoporation is the transient permeabilisation and resealing of a cell membrane with the help of ultrasound and/or an ultrasound contrast agent. We studied the behaviour of ultrasound contrast agent microbubbles near cancer cells at low acoustic amplitudes. After administering an ultrasound contrast agent, HeLa cells were subjected to 6.6-MHz ultrasound with a mechanical index of 0.2 and observed with a high-speed camera. Microbubbles were seen to enter cells and rapidly dissolve. We demonstrated that lipid-shelled microbubbles can be forced to enter cells at a low mechanical index. Hence, if a therapeutic agent is added to the shell of the bubble or inside the bubble, ultrasound-guided delivery could be facilitated at diagnostic settings. In addition, these results may have implications for the safety regulations on the use of ultrasound contrast agents for diagnostic imaging.

---

## 1. Introduction

The use of ultrasound for non-invasive diagnostics in both industry and medical imaging has proven itself to be invaluable due to its low price per examination and ease of use [1, 2, 3, 4].

In medical-diagnostics, guidelines state an  $MI < 0.3$  can be considered safe for pregnant women and neonatals, but yet diagnostic imaging machines allow the use of  $MI$  up to 1.9, putting the acoustic intensity used at the examiners discretion. The current regulations are based on the likelihood of inertial cavitation. It is known that inertial cavitation can cause damage not only to cells but also to metals, such as boat propellers and car injectors [5, 6, 7, 8]. Due to technical challenges, studying the formation and interaction of ultrasound generated cavities is minimal. Therefore the current understanding the consequences of cavitation near or inside cells is limited.

Previous studies on non-invasive, ultrasound-induced therapeutics used acoustic amplitudes corresponding to mechanical indices between 0.2 and 7.0 [9, 10, 11].

We analysed the manufacture of efficient, high-frequency, HIFU transducers, capable of high-resolution tissue ablation. It was shown that these transducers could be manufactured at low material cost ( $< \pounds 25$ ) compared to commercial HIFU PZT transducers, yet these low-budget transducers were capable of generating acoustic amplitudes equivalent to an  $MI > 3.0$ . Furthermore, single-element high-frequency high-intensity transducers cost even less ( $< \pounds 7$  in material costs) to manufacture. These transducers were capable of acoustic amplitudes equivalent to an  $MI = 2.7$  at a centre transmit frequency of 6.6 MHz, and worked up to the 5<sup>th</sup> harmonic of 35 MHz, generating a sound field equivalent to an  $MI = 0.4$ . These transducers surpassed the safety threshold for diagnostic use even at the 5<sup>th</sup> harmonic.

In addition to being economic and time effective, these transducers were also more environmentally friendly when compared to traditional piezo-ceramics, as the piezo-electric crystal used was lead-free and did not require poling.

A limitation in the use of  $\text{LiNbO}_3$  as a piezo-electric element is its fragility. The  $\text{LiNbO}_3$  elements were seen to be very sensitive to stress concentrations and tended to crack when small physical loads were applied in comparison to PZT piezo-ceramics, *e.g.*, when lapping or dicing to the desired thickness or shape. This fragility was also noticed when applying a high voltage over these elements. For this reason, higher tolerances need to be used when manufacturing transducers with  $\text{LiNbO}_3$  active elements. In addition  $\text{LiNbO}_3$  is a very poor receiver compared to traditional PZTs due to its low  $d_{33}$  value, thus it can't be used for imaging and diagnostics.

High-frequency transducers capable of FUS would allow for smaller lesion formation which might surpass the precision of invasive surgery, whilst avoiding the risks associated with invasive surgery [12]. Affordable transducers capable of high-resolution FUS will open a whole new field in ultrasound-induced therapeutics.

We have shown that coagulative necrosis can occur in less than 90 seconds at an  $MI < 2.0$  [13], and cellular damage can occur in the presence of microbubbles at an  $MI < 0.2$  [14].

Low- $MI$  ultrasound fields were used to study ultrasound contrast agents in artificial capillaries. We showed that continuous 2.2-MHz and 7.0-MHz ultrasound at an  $MI < 0.015$  formed clusters of more than 2000 microbubbles at precise locations. This cluster-formation phenomenon might be used to purposely block vessels, *e.g.*, to temporarily stop blood supply to a tumour, or to gather drug-loaded microbubbles to a specific location for ultrasound-enhanced drug delivery.

The formation of such clusters only occurred at high microbubble concentrations, *i.e.*, at concentrations only theoretically feasible in the human body with undiluted bolus injections. The influence of the flow rate to cluster formation has to be investigated.

To understand the effects of high-intensity ultrasound in tissue, we need to improve our understanding of acoustic cavitation. Acoustic cavitation typically occurs within a few acoustic cycles at unpredictable locations. To study cavitation with high-speed photography, we need to precisely know the site of nucleation. We describe a scientific instrument that is dedicated to this outcome, combining a focussed ultrasound transducer with a pulsed laser [15]. We demonstrated that inertial cavitation can be controllably introduced to the ultrasound focus. Acoustic cavitation was seen to occur at acoustic amplitudes equivalent to an  $MI = 0.7$ . At higher  $MI$ , dynamic cavitation clouds were formed. Our

findings will contribute to the understanding of cavitation evolution in focussed ultrasound, including for potential therapeutic applications.

All previous sonoporation publications involved high-MI ultrasound to deliver compounds into cells. Here we explored low-MI methods for drug and gene delivery.

## 2. Methodology

An overview of the experimental setup is shown in Figure 1. We have described our experimental setup extensively in Delalande *et al.* [14]. In short, a signal consisting of 40 cycles with a centre frequency of 6.6 MHz and a pulse repetition frequency of 10 kHz, was generated by an AFG 3102, dual channel arbitrary function generator (Tektronix, Inc., Beaverton, OR), amplified by a 2100L, 50-dB RF amplifier (Electronics & Innovation Ltd., Rochester, NY) and fed to a custom-built 6.6-MHz ultrasound transducer with a hexagonal Y-36° lithium niobate element with a maximum diameter of 25 mm [13]. The peak-negative acoustic pressure corresponds to an MI of 0.2. The transducer was placed in a custom-built, 260 × 160 × 150 (mm)<sup>3</sup> Perspex sonication chamber, in which an OptiCell<sup>®</sup> cell culture chamber (Nunc GmbH & Co. KG, Langenselbold, Germany) was placed. One side of the cell culture chamber contained a monolayer of HeLa cells. Ultrasound contrast agent was injected into the cell culturing chamber before each experiment.

A customised BAXFM-F microscope unit with an LC Ach N 20×/0.40 NA PhC (Olympus Deutschland GmbH, Hamburg, Germany) and a LUMPlanFL 60×/0.90 NA water-immersion objective (Olympus) was placed on top of the sonication chamber with the objective lens immersed in the water. The colour charge coupled device (CCD) of a PHOTRON FastCam MC-2.1 high-speed camera (VKT Video Kommunikation GmbH, Pfullingen, Germany) was connected to the microscope.

## 3. Results and Discussion

Lipid-shelled microbubbles were forced into cells using pulsed ultrasound at MI=0.2 at transmit frequencies of 1.0 MHz and 6.6 MHz. This phenomenon typically takes 2 s from the moment a bubble contacts the cell membrane, to complete dissolution of the gas inside the cell. Most bubble–cell penetration occurred within 8 s from the start of sonication. These results were easily reproducible, independent of the setup geometry. We are the first to observe the translation of entire microbubbles into cells. Since bubbles can be forced into cells, release mechanisms to detach drugs from microbubbles may be of lesser importance. Figure 2 shows an event resampled at 500 Hz. Here a 2 µm bubble penetrates the cancer cell at  $t = 4.404$  s, where  $t = 0$  s denotes the start of sonication. In Figure 3 shows the same event resampled at 25 Hz. The 2 µm bubble completely dissolved 2 s after it penetrated the cell. Targeted drug delivery down to the cellular level, with the use of encapsulated bubbles will allow the use of high-toxicity drugs to be injected into the body, but only delivered to a specific area. Thus, leaving healthy tissue unaffected.

Our sonoporation observations could be attributed to the long pulse lengths used. The bubble–cell attraction then may be attributed to secondary Bjerknes forces, similar to those described Kottopoulis and Postema [16]. In diagnostic imaging, much shorter pulse lengths are used. Although cells themselves are acoustically active, this acoustic activity is probably negligible to that of microbubbles in high concentrations. Therefore, we expect bubble–cell interaction to be more likely in very low bubble concentrations. This type of bubble–cell attraction is less likely to occur using common clinical diagnostic equipment.

We have shown that it is possible to manufacture low-cost therapeutic transducers. Ultrasound can be used to kill single cancer cells or increase drug uptake. We have managed to induce acoustic cavitation at precise locations

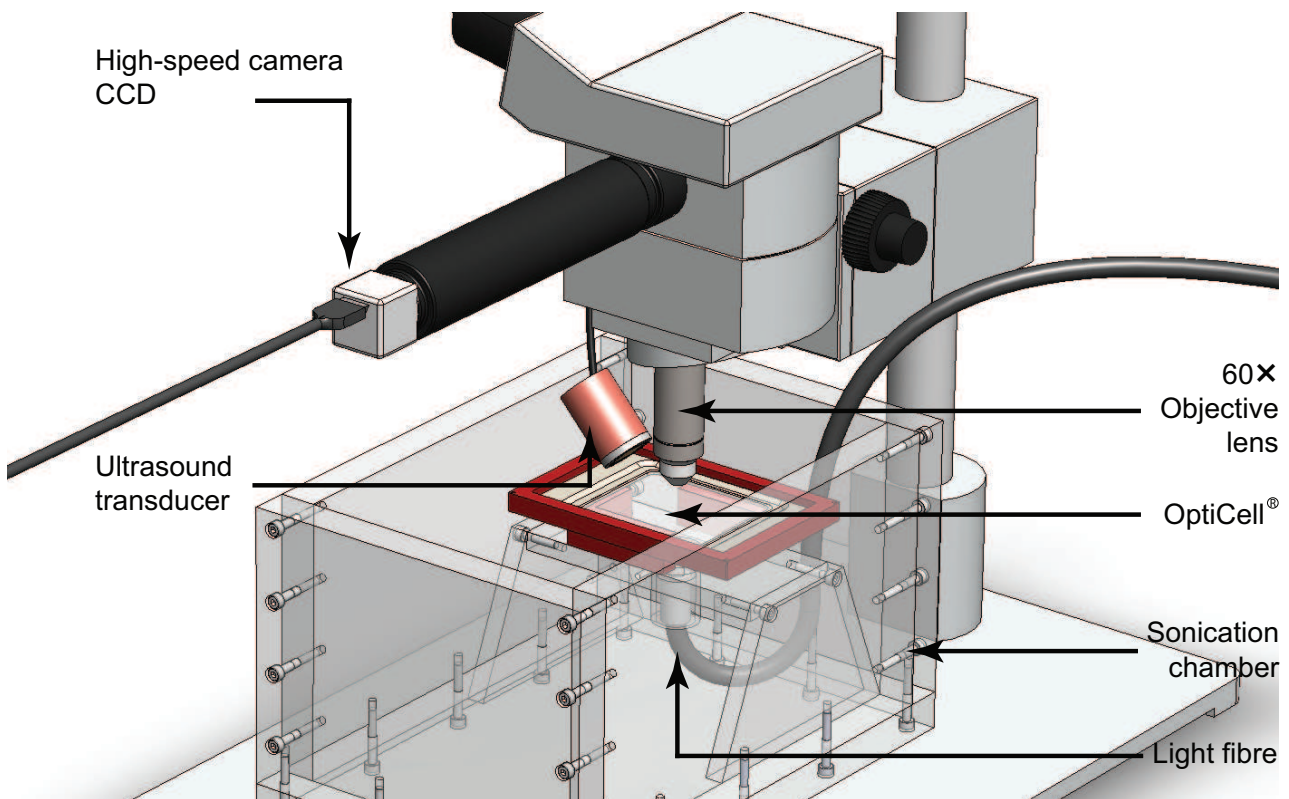
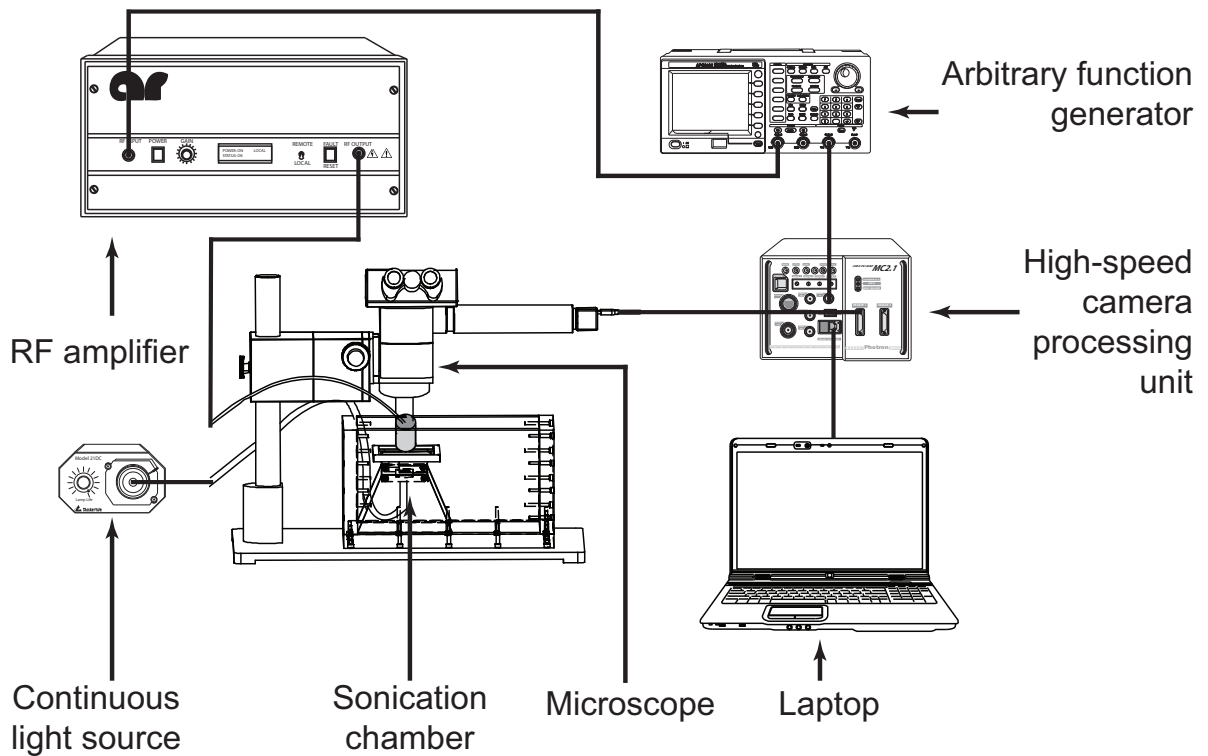


**Figure 1.** Experimental setup (*top*) and a close-up of the sonoporation configuration (*bottom*).

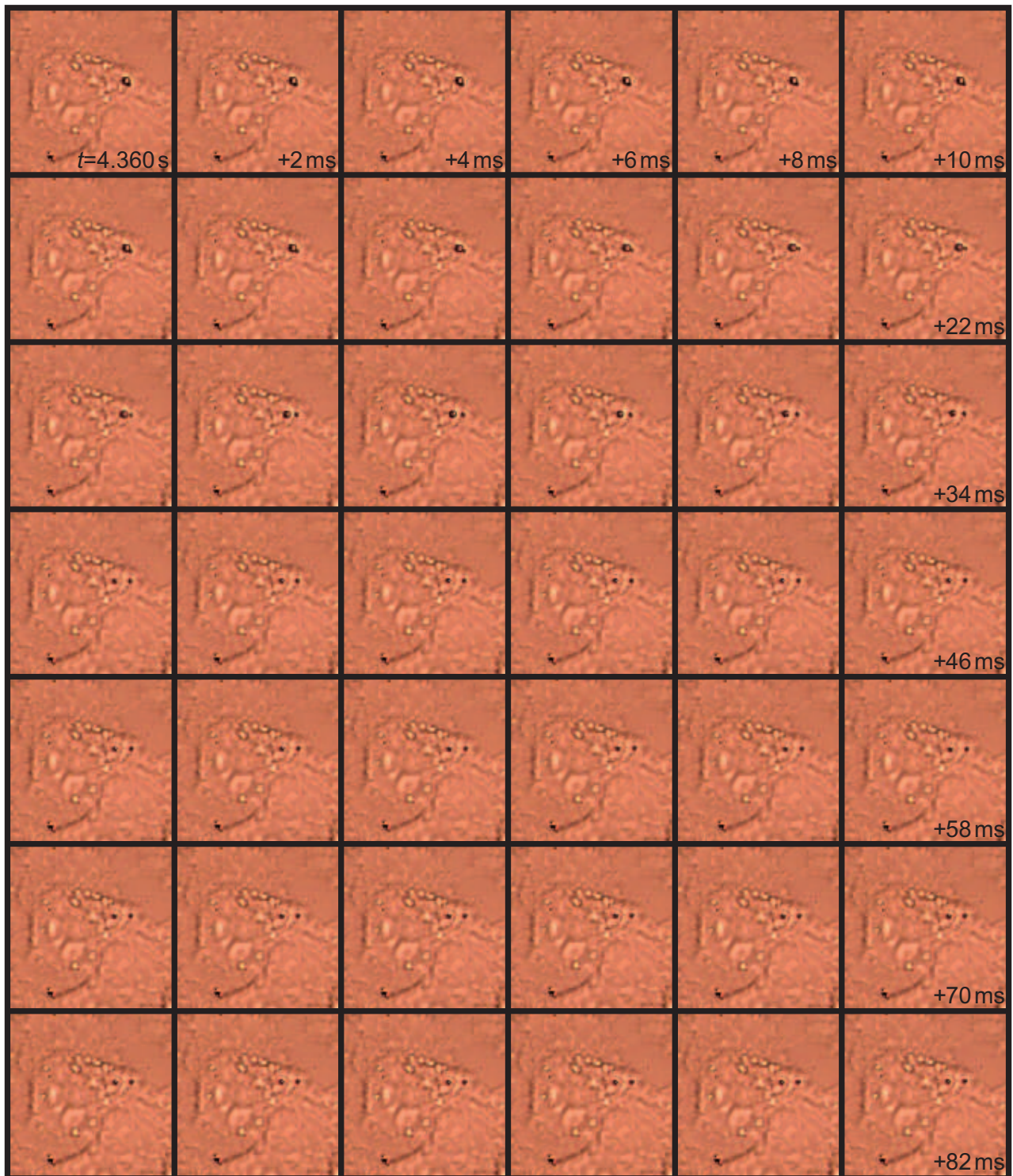


**Figure 2.** A sonoporation event resampled at 500 Hz where  $t = 0$  s denotes the start of sonication. The  $2 \mu\text{m}$  bubble enters the cell at  $t = 4.404$  s. Each frame corresponds to a  $20 \times 20 (\mu\text{m})^2$  area.

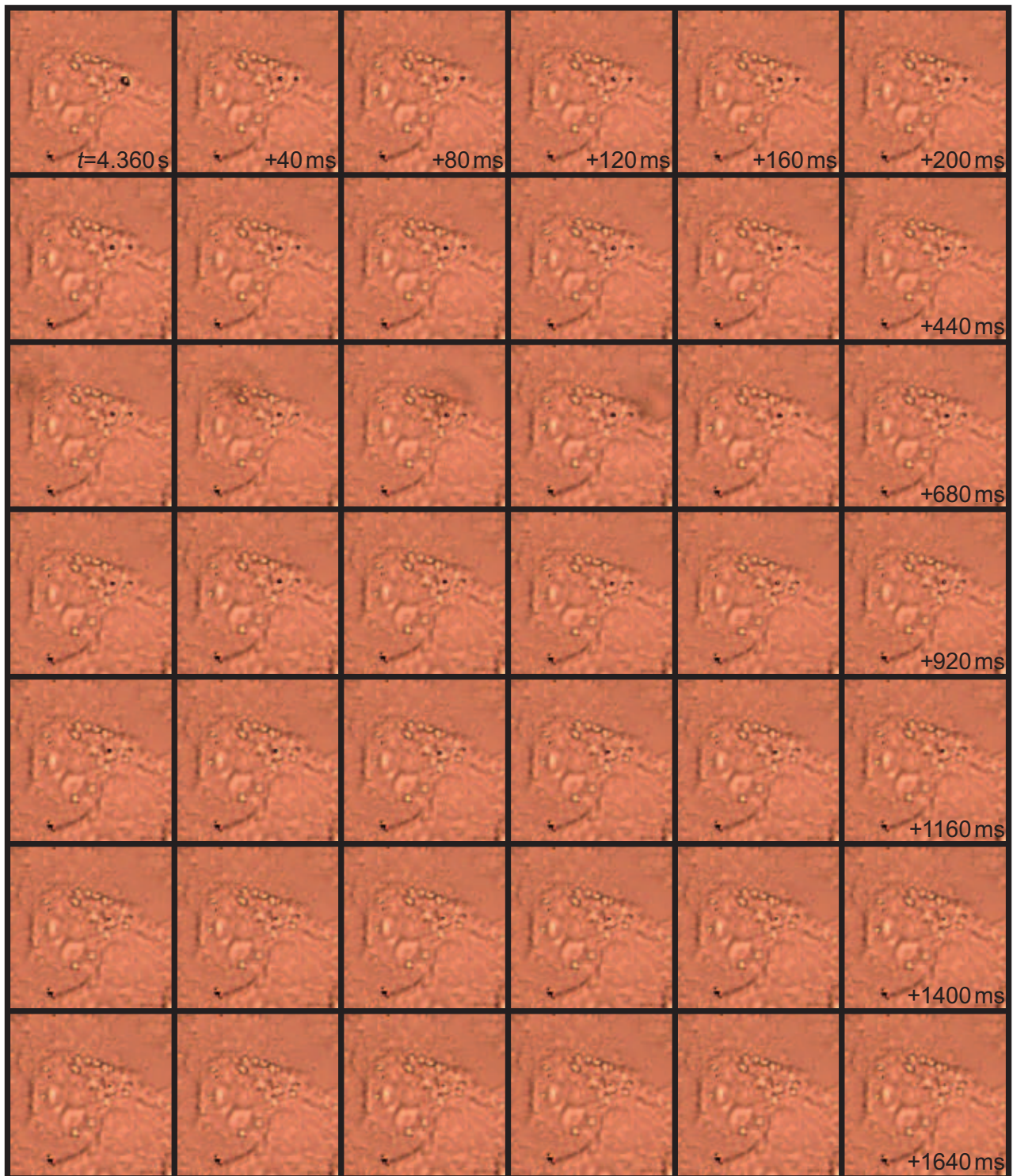


**Figure 3.** A sonoporation event resampled at 25 Hz where  $t = 0$  s denotes the start of sonication. The  $2 \mu\text{m}$  bubble enters the cell at  $t = 4.404$  s and completely dissolves 2 s after penetration. Each frame corresponds to a  $20 \times 20 (\mu\text{m})^2$  area.

## 4. Future work

To ensure reliable performance of LiNbO<sub>3</sub> transducers, several flaws must be addressed. As the Ag-paint electrodes were damaged due to heat and cavitation at the electrode–crystal interface, different electrode materials need to be investigated, *e.g.*, Cr-Au or Ti-Pt. In addition to more reliable electrode application techniques need to be explored. Sputter coating thin film electrodes should eliminate gas pockets at the electrode–crystal interface, leading to better coupling, thus less crystal heating. Other improvements include transducer designs where the natural foci of each active element could be aligned more accurately, lighter support materials, and protective outer layers

Our preliminary laser-nucleated acoustic cavitation results show the formation of cavitation clouds at high MI. Very little is known on the dynamics of cavitation clouds. Because clouds are easily induced, their role in FUS must be studied.

We still need to assess the viability of cells penetrated by microbubbles, and subsequently evaluate the suitability of this sonoporation technique for localised drug delivery. This, of course, requires therapeutics to be incorporated in the microbubbles. Although encapsulation processes go beyond the scope of this paper, they are essential to the future success of ultrasound-guided drug and gene delivery. If drug and genes can be successfully coupled to acoustically active vehicles, sonoporation might revolutionise non-invasive therapy as we know it.

## REFERENCES

- <sup>1</sup> Houze M, Nonailard B, Gazalet M, Rouvaen J, and Bruneel C, Measurement of the thickness of thin layers by ultrasonic interferometry, *J Appl Phys* **55**(1), 194–198 (1984).
- <sup>2</sup> Tiu CM, Chou YH, Chen JD, Chiou YY, Chiou SY, Wang HK, Chen SP, Wei CF, and Chin TW, Ultrasound diagnosis of acute appendicitis: impact on cost and outcome in pediatric patients, *J Med Ultrasound*, **12**(3), 69–74 (2004).
- <sup>3</sup> Courtney C, Drinkwater B, Neild S, and Wilcox P, Factors affecting the ultrasonic intermodulation crack detection technique using bispectral analysis, *NDT & E Int* **41**, 223–234 (2008).
- <sup>4</sup> Vachhani M, Hamer F, and Clarke F, Cost effectiveness of ultrasound scan by middle grade doctors in Gynaec Assessment Unit (GAU), *Int J Gynecol Obstet* **107**(2), S470 (2009).
- <sup>5</sup> Palanker D, Vankov A, Miller J, Friedman M, and Strauss M, Prevention of tissue damage by water jet during cavitation, *J Appl Phys* **94**(4) 2654–2661 (2003).
- <sup>6</sup> Fuciarelli A, Sisk E, Thomas R, and Miller D, Induction of base damage in DNA solutions by ultrasonic cavitation. *Free Radic Biol Med* **18**(2) 231–238 (1995).
- <sup>7</sup> Gerr D, Ed., *The Propeller Handbook: The complete reference for choosing, installing, and understanding boat propellers*, Maidenhead: McGraw-Hill (2001).
- <sup>8</sup> Asi O, Failure of diesel engine injector nozzle by cavitation, *Eng Fail Anal* **13**(7) 1126–1133 (2006).
- <sup>9</sup> Deng CX, Pan S, and Cui J, Ultrasound-induced cell membrane porosity, *Ultrasound Med Biol* **30** 519–526 (2004).
- <sup>10</sup> Pua E and Zhong P, Ultrasound-mediated drug delivery. *IEEE Eng Med Biol* **28**(1) 64–75 (2009).
- <sup>11</sup> Bigelow T, Northagen T, Hill T, and Sailer F, The destruction of escherichia coli biofilms using high-intensity focussed ultrasound, *Ultrasound Med Biol* **35**(6) 1026–1031 (2009).



- <sup>12</sup> Hakim N and Papalois V, *Surgical Complications: Diagnostics and Treatment*. London: Imperial College Press (2007).
- <sup>13</sup> Kotopoulis S, Wang H, Cochran S, and Postema M, Lithium niobate transducer for MRI-guided ultrasonic microsurgery, *IEEE Trans Ultrason Ferroelectr Freq Control* accepted (2011).
- <sup>14</sup> Delalande A, Kotopoulis S, Rovers T, Pichon C, and Postema M, Sonoporation at a low mechanical index, *Bub Sci Eng Tech* **3(1)** accepted (2011).
- <sup>15</sup> Gerold B, Kotopoulis S, McDougall C, M<sup>c</sup>Gloin D, Postema M, and Prentice P, Laser-nucleated acoustic cavitation in focussed ultrasound, *Rev Sci Instrum* accepted (2011).
- <sup>16</sup> Kotopoulis S and Postema M, Microfoam formation in a capillary, *Ultrasonics* **50(2)** 260–268 (2010).